

This is a repository copy of *GFP fusions of Sec-routed extracellular proteins in _Staphylococcus aureus_ reveals surface-associated coagulase in biofilms.*

White Rose Research Online URL for this paper:

<https://eprints.whiterose.ac.uk/201747/>

Version: Accepted Version

Article:

Evans, Dominique, Khamas, Amanda B, Marcussen, Lisbeth et al. (7 more authors)
(Accepted: 2023) GFP fusions of Sec-routed extracellular proteins in *_Staphylococcus aureus_* reveals surface-associated coagulase in biofilms. *Microbial Cell*. ISSN 2311-2638
(In Press)

Reuse

Items deposited in White Rose Research Online are protected by copyright, with all rights reserved unless indicated otherwise. They may be downloaded and/or printed for private study, or other acts as permitted by national copyright laws. The publisher or other rights holders may allow further reproduction and re-use of the full text version. This is indicated by the licence information on the White Rose Research Online record for the item.

Takedown

If you consider content in White Rose Research Online to be in breach of UK law, please notify us by emailing eprints@whiterose.ac.uk including the URL of the record and the reason for the withdrawal request.

1 GFP fusions of Sec-routed extracellular proteins in *Staphylococcus aureus* reveals surface-
2 associated coagulase in biofilms

3 Dominique C. S. Evans^{1,3,*}, Amanda B. Khamas^{1,*}, Lisbeth Marcussen¹, Kristian S. Rasmussen²,
4 Janne K. Klitgaard², Birgitte H. Kallipolitis², Janni Nielsen¹, Daniel E. Otzen¹, Mark C. Leake^{3,4} [♣],
5 Rikke L. Meyer^{1,5*}

6
7 ¹Interdisciplinary Nanoscience Centre, Aarhus University, Aarhus, Denmark

8 ²Department of Biochemistry and Molecular Biology, University of Southern Denmark, Odense,
9 Denmark

10 ³Department of Physics, University of York, York, UK

11 ⁴Department of Biology, University of York, York, UK

12 ⁵Department of Biology, Aarhus University, Aarhus, Denmark

13 *Joint first authors

14 [♣]Corresponding authors: rikke.meyer@inano.au.dk; mark.leake@york.ac.uk

15 Rikke L. Meyer¹ is designated to correspond with Microbial Cell: rikke.meyer@inano.au.dk, +45
16 60202794

17 Keywords: Fusion protein, Gram positive bacteria, monomeric superfolder GFP, coagulase,
18 biofilms

19 Running title: msfGFP for labelling secreted proteins in *S. aureus*

20 REVISION. Manuscript number: MIC0272E143. Original manuscript title: Monomeric superfolder
21 GFP can be used to label Sec-routed extracellular proteins in *Staphylococcus aureus* and reveals
22 surface-associated coagulase in biofilms

23

24 **ABSTRACT**

25 *Staphylococcus aureus* is a major human pathogen that utilises many surface-associated and
26 secreted proteins to form biofilms and cause disease. However, our understanding of these
27 processes is limited by challenges of using fluorescent protein reporters in their native environment,
28 because they must be exported and fold correctly to become fluorescent. Here, we demonstrate the
29 feasibility of using the monomeric superfolder GFP (msfGFP) exported from *S. aureus*. By fusing
30 msfGFP to signal peptides for the Secretary (Sec) and Twin Arginine Translocation (Tat) pathways,
31 the two major secretion pathways in *S. aureus*, we quantified msfGFP fluorescence in bacterial
32 cultures and cell-free supernatant from the cultures. When fused to a Tat signal peptide, we detected
33 msfGFP fluorescence inside but not outside bacterial cells, indicating a failure to export msfGFP.
34 However, when fused to a Sec signal peptide, msfGFP fluorescence was present outside cells,
35 indicating successful export of the msfGFP in the unfolded state, followed by extracellular folding
36 and maturation to the photoactive state. We applied this strategy to study coagulase (Coa), a
37 secreted protein and a major contributor to the formation of a fibrin network in *S. aureus* biofilms
38 that protects bacteria from the host immune system and increases attachment to host surfaces. We
39 confirmed that a genomically integrated C-terminal fusion of Coa to msfGFP does not impair the
40 activity of Coa or its localisation within the biofilm matrix. Our findings demonstrate that msfGFP
41 is a good candidate fluorescent reporter to consider when studying proteins secreted by the Sec
42 pathway in *S. aureus*.

43

44 **INTRODUCTION**

45 Green fluorescent protein (GFP) has been used for decades as an intracellular reporter for gene
46 expression and as a fluorescent tag to visualise single proteins in the cytoplasm of bacteria [1]. An
47 advantage of fluorescent proteins is that samples do not need to be stained and incubated to
48 visualise the protein. GFP and other fluorescent proteins have therefore been instrumental for
49 studies into protein localisation, visualising subcellular compartments, monitoring gene expression,
50 tissue labelling, as well as DNA and RNA labelling [2].

51 While GFP fusion proteins have taught us much about intracellular proteins, little research
52 has been done on extracellular proteins, such as surface-bound proteins or other secreted proteins.
53 Some GFP variants have been successfully secreted to the periplasm and outer membrane of Gram-
54 negative bacteria [3][4][5], however there are only few examples of this for Gram-positive bacteria.
55 To our knowledge, GFP secretion in Gram-positive bacteria has only been achieved in a small
56 number of organisms, including *Corynebacterium glutamicum* [6], *Bacillus subtilis* [7][8],
57 *Streptococcus mutans* [9], *Mycobacterium smegmatis* [10], and *Staphylococcus epidermidis* [11].
58 Split GFP has additionally been successfully secreted by *B. subtilis* [12]. There is a multitude of
59 reasons why generation of GFP-fusion proteins may fail. In particular, the fusion protein may not be
60 successfully secreted, the GFP may misfold and fail to become fluorescent in the extracellular
61 environment, or the chromophore may not mature properly [6][13]. Additionally, the level of
62 transcription and translation, protein turnover rate, and photobleaching further complicate imaging
63 of GFP fusions [13].

64 Most extracellular proteins are secreted in an unfolded state via the Secretory (Sec) pathway,
65 where they are exported across the cytosolic membrane into the periplasm in Gram-negative

66 bacteria or outside the cell in Gram-positive bacteria [14]. It is a highly conserved pathway present
67 in all classes of bacteria [15]. Sec-routed proteins have a signal peptide at their N-terminus that
68 directs them towards the SecYEG membrane protein channel, after which they are driven stepwise
69 across the membrane by the ATPase molecular motor SecA [16]. The transported protein then folds
70 on the trans side of the membrane. In many Gram-negative bacteria, SecB stabilises and targets the
71 unfolded protein to SecA, while in Gram-positive and other Gram-negative bacteria, general
72 chaperones maintain the protein in an unfolded state [16]. Another common secretion pathway is
73 the Twin Arginine Translocation (Tat) pathway, in which proteins are exported in a folded state
74 [17], however not all bacterial species have a Tat pathway [18]. Tat-routed proteins have an N-
75 terminal signal sequence containing a twin-arginine motif that gives the pathway its name [19].
76 Some proteins that are secreted through the Tat-pathway, such as proteins with co-factors that bind
77 to cytoplasmic proteins, usually need to fold in the cytoplasm to function correctly [20]. The Tat
78 pathway contains three subunits TatA, TatB, and TatC in Gram-negative bacteria and two subunits
79 TatA and TatC in Gram-positive bacteria, which bind the signal peptide and form a membrane
80 spanning channel [15]. These subunits have been studied previously using fluorescent protein
81 reporters in live *Escherichia coli* cells [21]. Folded proteins are exported outside of the cell in
82 Gram-positive bacteria, and to the periplasm in Gram-negative bacteria, where they may be
83 exported across the outer membrane via other mechanisms [15].

84 The aims of our present study were to investigate whether monomeric superfolder GFP
85 (msfGFP) is a good candidate for extracellular fusion proteins in *Staphylococcus aureus*, and to
86 determine if msfGFP can be secreted by either of the two secretion pathways Sec and Tat. *S. aureus*
87 is a Gram-positive coccus which has both the Sec and Tat secretion pathways [15][18]. It is a major
88 biofilm-forming human pathogen that can cause skin and soft tissue infections, endocarditis,
89 osteomyelitis, and toxic shock syndrome [22]. *S. aureus* utilises many surface-associated and

90 secreted proteins to interact with host tissue, to establish infections, and evade the immune system
91 [23]. These proteins include a family known as microbial surface components recognising adhesive
92 matrix molecules (MSCRAMMs), all of which contain a Sec signal peptide [23]. Examples include
93 clumping factors A and B (ClfA and ClfB) that clump bacteria by binding host fibrinogen and aid
94 tissue colonisation [24], fibronectin binding proteins A and B (FnBPA and FnBPB) that bind host
95 fibronectin, fibrinogen, and elastin, and therefore facilitate attachment to host tissues via host
96 proteins [24], and collagen adhesin (Cna) that facilitates attachment via collagen and helps *S.*
97 *aureus* escape immune cells [23]. *S. aureus* also secretes a family of proteins called secretable
98 expanded repertoire adhesive molecules (SERAMs). These include extracellular adherence protein
99 (Eap), extracellular matrix protein-binding protein (Emp), extracellular fibrinogen binding protein
100 (Efp), coagulase (Coa), and von Willebrand factor binding protein (vWbp). Eap inhibits neutrophils
101 and therefore inhibits the immune response [25], Emp binds host fibronectin, fibrinogen, and
102 vitronectin [26], which appears to be important for virulence [26], and Efp inhibits phagocytosis
103 [27] and decreases wound healing [28]. Coa and vWbp bind to and activate host prothrombin to
104 hijack the host coagulation cascade and thereby triggering the formation of fibrin fibers, a major
105 component of the biofilm extracellular matrix [29], in two concentric structures: a cell surface-
106 associated pseudocapsule and an extended outer network, which together act as mechanical barriers
107 against immune attack [30], enhance virulence [31], and increase adhesion to surfaces [32]. *S.*
108 *aureus* would benefit from a reliable system with which to label and visualise proteins such as these
109 that are important to its virulence and pathogenicity, especially in complex environments such as
110 biofilms where traditional antibody labelling methods may fail. Antibodies are approximately 10
111 nm in size [33], which is relatively large compared to many matrix components, such as DNA
112 which has a width of approximately 2.5 nm and many proteins which are less than 10 nm in size.
113 Therefore antibodies may fail to penetrate some biofilm matrices and fail to label them correctly.

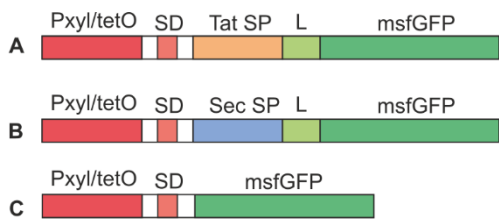
114 We chose msfGFP as our model fluorescent protein due to its brightness and enhanced
115 folding properties [34], and it has been previously shown to fold in traditionally challenging
116 environments such as the periplasm of Gram-negative bacteria [34]. We investigated Sec- and Tat-
117 secreted msfGFP by fusing msfGFP to Sec and Tat signal peptides in overexpression plasmids and
118 subsequently measuring the increase in fluorescence from bacterial cultures and cell-free culture
119 supernatants. After confirming that msfGFP is suitable to visualise secreted proteins, we developed
120 a C-terminal chromosome-integrated fusion between msfGFP and Coa in *S. aureus*, which is
121 predicted to have a Sec-type signal peptide [35]. We demonstrated that fusion to msfGFP did not
122 impair the biological function of Coa, and that Coa:msfGFP fusion proteins revealed the location of
123 Coa in *S. aureus* biofilms. Coa is responsible for producing a fibrin pseudocapsule and has
124 previously been located within the pseudocapsule [30][31]. We demonstrate that Coa localises to
125 cell surfaces, where we hypothesise that it associates with the cell to facilitate fibrin production near
126 the surface of bacteria.

127

128 **RESULTS**

129 **msfGFP is secreted via Sec and becomes fluorescent in the extracellular environment**

130 The fluorescent protein msfGFP is a good candidate for tagging extracellular proteins in Gram-
131 positive bacteria, but its implementation depends on whether it can be secreted and fold properly in
132 the extracellular space. We therefore tested the ability of msfGFP to become fluorescent after
133 secretion via the Tat and Sec pathways in *S. aureus*. We generated four strains of *S. aureus* that
134 carried different variants of the overexpression pRMC2 plasmid (Figure 1). Strain 1 contained an
135 empty pRMC2 vector, which served as negative control, strain 2 contained pRMC2 encoding
136 msfGFP without a signal peptide and was used as a positive control to verify msfGFP expression,



Sec SP: MKKCIKTLFLSILVVMMSGWYHSAHA

Tat SP: MTNYEQVNDSTQFSRRTFLKMLGIGGAGV
AIGA

Linker: SGGGG

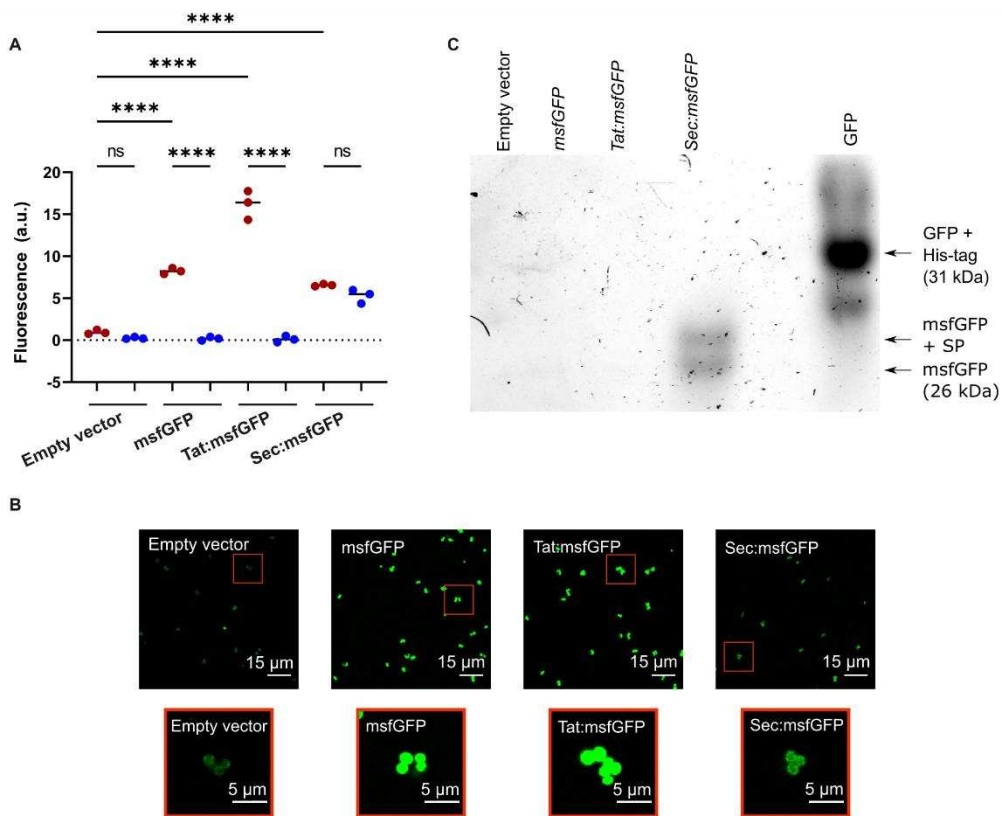
137

138 Figure 1 Visual schematics of constructs expressing fusion proteins under control of the inducible
 139 $P_{\text{xyI/tetO}}$ promoter in pRMC2. a) Tat:msfGFP, b) Sec:msfGFP, and c) msfGFP control. SD = Shine-
 140 Dalgarno sequence, SP = signal peptide, and L = linker. Amino acid sequences for the Tat signal
 141 peptide [18], Sec signal peptide [45] and linker are given in the figure. DNA sequences are provided
 142 in Supplementary S1.

143

144 strain 3 contained pRMC2 encoding Tat:msfGFP for secretion of GFP through the Tat pathway, and
 145 strain 4 contained pRMC2 encoding Sec:msfGFP for secretion through the Sec pathway. The
 146 presence of functional msfGFP was then measured as the appearance of green fluorescence of
 147 cultures and cell-free supernatants using a fluorescence plate reader after inducing expression of
 148 msfGFP from the plasmid.

149 Only the culture expressing Sec:msfGFP produced fluorescence in the cell-free supernatant,
 150 which indicated that msfGFP can secrete and fold correctly when exported by the Sec-pathway
 151 (Figure 2a). The fluorescence intensity from the culture (bacteria and supernatant) was at a similar
 152 level to the supernatant alone, indicating that msfGFP was primarily present in the supernatant. In
 153 cultures expressing Tat:msfGFP or msfGFP without a signal peptide, fluorescence was detected in
 154 bacterial cultures but not the supernatants (Figure 2a), indicating that msfGFP could fold correctly



155

156 Figure 2 a) Fluorescence intensity from excitation of msfGFP in cell cultures (red circles) or cell-
 157 free supernatants (blue circles) of *S. aureus* expressing msfGFP from the pRMC2 vector. msfGFP
 158 was fused to either Tat or Sec signal peptides, no signal peptide, or not expressed at all (empty
 159 vector). Black bars indicate group medians. Samples were compared using a one-way ANOVA
 160 followed by a Tukey's test; **** denotes a $p < 0.0001$ significance level and ns denotes no
 161 significance. b) CLSM images of *S. aureus* cells expressing msfGFP fusions. Red boxes indicate
 162 zoomed in images. All fluorescence images had their brightness increased equally using Fiji ImageJ
 163 for clear visualisation. c) In-gel fluorescence of GFP/msfGFP in a native PAGE gel containing
 164 supernatants from cultures expressing empty pRMC2 vector, msfGFP without signal peptide or
 165 fused to either sec or tat signal peptide.

166

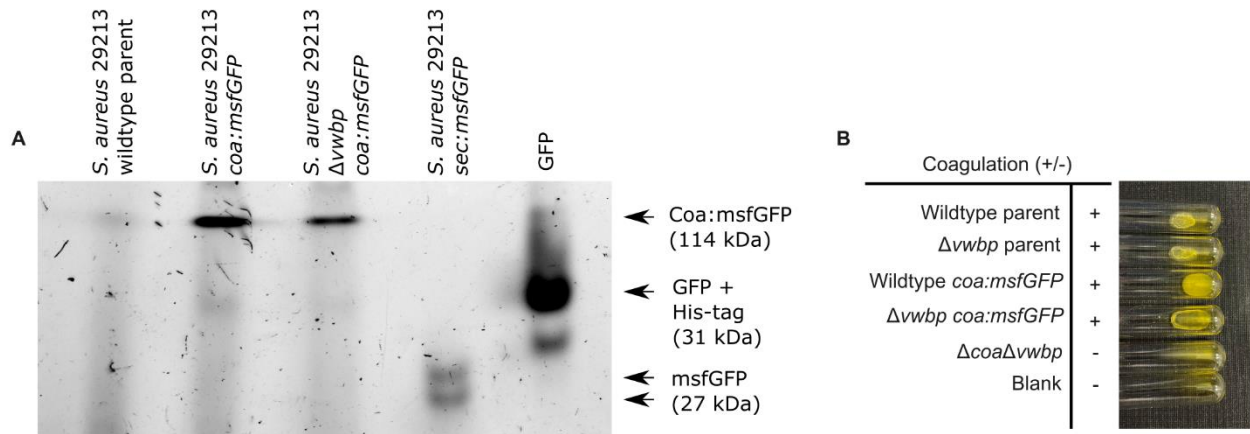
167 within cells, but was not secreted via the Tat pathway. Although Tat:msfGFP was not successfully
168 secreted, the fluorescence intensity from Tat:msfGFP cell cultures was higher than the fluorescence
169 intensity from Sec:msfGFP cell cultures, which may reflect differences in the activity of the two
170 different pathways, different rates of msfGFP transcription, translation, or protein folding when
171 fused to a particular signal peptide.

172 The presence of fluorescent msfGFP in the intracellular and extracellular environment was verified
173 by CLSM imaging of cell cultures expressing Tat:msfGFP, Sec:msfFP, msfGFP, and cells
174 containing the empty vector. As expected, msfGFP fluorescence was detected inside cells
175 expressing Tat:msfGFP and msfGFP (Figure 2b). There was a weak fluorescence in *S. aureus*
176 expressing Sec:msfGFP, which reflects that there was a small fraction of GFP that was not secreted
177 from the bacteria or that remained linked to the cell wall. Furthermore, in-gel fluorescence showed
178 that only the Sec:msfGFP strain secreted a functional msfGFP (Figure 2c). However, the secreted
179 msfGFP was found in two distinct sizes in the supernatant of the Sec:msfGFP cultures, which
180 indicates that the signal peptide was not always removed from some of the msfGFP during
181 secretion. There is an additional band underneath the GFP control (Figure 2c), which is likely GFP
182 that lacks a His-tag. Although we have confirmed msfGFP is found in the supernatant by bulk
183 measurements using a plate reader (Figure 2a), the fluorescence could not be seen in the supernatant
184 using CLSM because the fluorescent protein was too diluted to be visualised. There is also a weak
185 surface-associated fluorescent signal seen with CLSM on *S. aureus* containing an empty vector
186 without msfGFP, which is due to autofluorescence from ATc [36].

187

188

189



190

191 Figure 3 The Coa:msfGFP fusion protein was successfully secreted from *S. aureus* and functioned
 192 correctly. a) In-gel fluorescence of GFP/msfGFP in a native PAGE gel containing supernatants
 193 from *S. aureus* wildtype parent strain, as well as *S. aureus* wildtype and *S. aureus* $\Delta vwbp$ both
 194 expressing Coa:msfGFP. His-tagged GFP and supernatant from the strain expressing Sec:msfGFP
 195 were also loaded to the gel to serve as a molecular marker and as a positive control for GFP and
 196 msfGFP fluorescence, respectively. The gel shows that Coa:msfGFP was secreted as an intact,
 197 fluorescent protein, giving a band at the expected weight of msfGFP and Coa combined [53]. b)
 198 Coagulation of *S. aureus* 29213 wildtype and $\Delta vwbp$ producing either Coa:msfGFP or unmodified
 199 Coa and *S. aureus* 29213 $\Delta coa\Delta vwbp$ after 24 hours incubation with human plasma at 37 °C. All
 200 strains producing Coa coagulated plasma, while the double mutant $\Delta coa\Delta vwbp$ did not.

201

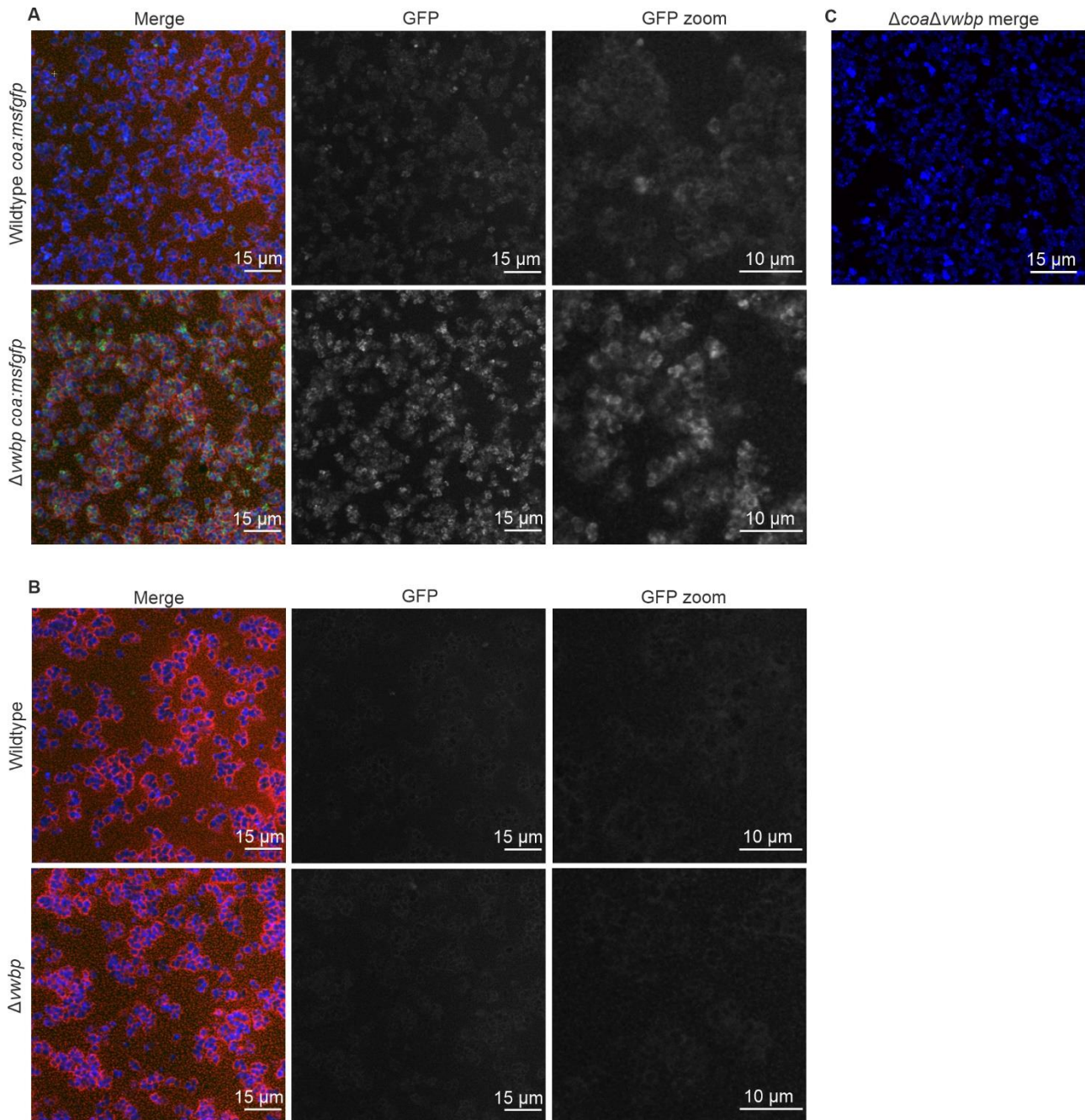
202 **Coa:msfGFP produces a functional coagulase that localises within the fibrin pseudocapsule**

203 msfGFP was successfully secreted via the Sec pathway, so to demonstrate its suitability to tag
 204 extracellular proteins, it was fused to Coa by insertion into the *S. aureus* chromosome via allelic
 205 exchange. Coa is one of two coagulases that hijack the human coagulation cascade and triggers the
 206 formation of a fibrin network around *S. aureus* cells, a major component of the biofilm extracellular
 207 matrix *in vivo*, that protects *S. aureus* from the host immune system during infection [29][30]. In

208 order to confirm that the chromosome-integrated *coa:msfGFP* had not impacted the ability of Coa
209 to cause coagulation, the fusion protein was first created in a mutant strain that lacks the other
210 coagulase: Von Willebrand factor binding protein (vWbp) [37]. Loss of function of coagulase
211 would then result in inability to coagulate plasma.

212 The fusion protein Coa:msfGFP was secreted successfully from *S. aureus* and the fusion
213 protein did not get cleaved, demonstrated by in-gel fluorescence analysis (Figure 3a). Fluorescence
214 from GFP was present in the supernatant of bacterial cultures expressing Coa:msfGFP and not in
215 cultures without Coa:msfGFP, demonstrating that the fusion protein was secreted extracellularly
216 (Figure 3a). Coa:msfGFP from the supernatant of bacterial cultures did not travel as far through the
217 gel as GFP alone, or msfGFP fused to a Sec signal peptide. Therefore, the weight of the fusion
218 protein was much larger, demonstrating that the protein is intact and contains both Coa and msfGFP
219 (Figure 3a). Coa was also functional, as *S. aureus* with chromosome-integrated *coa:msfGFP*
220 coagulated plasma similarly to the parental strains (Figure 3b), and biofilms formed similar fibrin
221 structures as the parental strains, i.e. fibrin was visible as pseudocapsules surrounding clusters of
222 bacteria and as an extended fibrous network between clusters of bacteria (Figure 4a, 4b). This was
223 true for both the wildtype and the mutant lacking vWbp, thus the fusion to msfGFP did not inhibit
224 the function of Coa. We confirmed that coagulation occurred due to Coa and vWbp alone by
225 including a control mutant of *S. aureus* that lacks both *coa* and *vwbp*, which did not coagulate
226 plasma (Figure 3b) nor produce fibrin fibers in the biofilm matrix (Figure 4c). Fibrin was visualised
227 by the addition of fluorescently labelled fibrinogen to the biofilm growth medium, which is
228 converted into fibrin fibers by an activated complex formed by Coa and vWbp binding to host
229 prothrombin. The small amount of red fluorescence seen in Figure 4c are aggregates of fluorescent
230 fibrinogen that have not been converted into fibrin because of the absence of both Coa and vWbp.

231



232

233 Figure 4 a) CLSM images of *S. aureus* wildtype and *S. aureus* $\Delta vwbp$ biofilms producing
 234 Coa:msfGFP. The composite image (left) is displayed along with the channel containing only signal
 235 from Coa:msfGFP (middle) and a zoomed in image of that channel (right). Coa:msfGFP localised
 236 to the surface of bacteria within the fibrin pseudocapsule. b) The parental strains of *S. aureus* that
 237 produce unmodified Coa when imaged with the same imaging settings as modified bacteria
 238 producing Coa:msfGFP. No fluorescence was detected, which confirms that the fluorescence in

239 Figure 4a originates from msfGFP and not from autofluorescence. c) A double mutant lacking both
240 Coa and vWbp ($\Delta coa\Delta vwbp$) forms no fibrin at all. Biofilms were grown in BHI containing 50 %
241 human plasma for 2 h. Bacteria (wildtype and $\Delta vwbp$) were visualised by staining with SYTO 41
242 (blue), fibrin was visualised by amending Alexa 647-conjugated fibrinogen to media (red), and Coa
243 was visualised by fluorescence emitted from msfGFP (green). The double mutant expressed *gfp*
244 from a plasmid pCM29 [54] (blue), and fibrin was also visualised by addition of Alexa-647-
245 conjugated fibrinogen to the media (red). Brightness for each colour channel for each image were
246 increased equally using Fiji ImageJ to visualise the data for both a) and b).

247

248 To assess the location of Coa in *S. aureus* biofilms, we visualised the bacterial cells, fibrin,
249 and Coa:msfGFP by CLSM. Coa:msfGFP localised to the surface of the bacteria, where we
250 predicted that Coa catalyses the formation of a fibrin pseudocapsule (Figure 4a). This finding
251 corroborates previous studies, which also detected Coa in the fibrin pseudocapsule by
252 immunolabelling [30]. Biofilms of the parental strain were used as negative controls, and here we
253 detected no fluorescence from GFP (Figure 4b). We have thus demonstrated the use of msfGFP for
254 labelling a protein secreted by the Sec pathway in *S. aureus*. The signal from msfGFP appears
255 brighter in the mutant lacking vWbp, and this is most likely caused by a less dense extracellular
256 matrix in this strain which lacks one of the coagulases, and the signal from msfGFP is therefore
257 attenuated less.

258

259 **DISCUSSION**

260 We show that msfGFP can be used to generate extracellular fluorescent fusion proteins in *S. aureus*,
261 but that the application is limited to proteins that are secreted through the Sec pathway. When fused

262 to Coa, msfGFP did not hinder the biological function of Coa, and the fusion protein localised to the
263 fibrin pseudocapsule surrounding clusters of *S. aureus* cells. This result is in agreement with
264 previous studies [30][31] and indicates that fusion to msfGFP does not cause Coa to mislocalise or
265 malfunction. Therefore, msfGFP is a good candidate for tagging *S. aureus* proteins exported by the
266 Sec pathway, and the majority of extracellular proteins are indeed secreted by this pathway [14].

267 msfGFP has a superfolding mutation that makes it fold quickly and without chaperones,
268 even when fused to another protein, and it exhibits a high level of brightness [34] that makes it ideal
269 for creating fusion proteins in the extracellular environment. Correct folding is essential for
270 chromophore formation and fluorescence, while fast folding is also important for the protein to fold
271 into its 3D conformation in time to avoid cleavage by extracellular proteases that clear unfolded or
272 misfolded proteins away from the cell surface. msfGFP is also monomeric, which makes it less
273 likely to aggregate and cause artefacts, which makes it a good candidate for many fusion proteins.
274 We have demonstrated for the first time the generation of fluorescent fusion proteins for a secreted
275 protein in *S. aureus*, and this approach now opens possibilities of studying the location of secreted
276 proteins that remain associated with the extracellular matrix of staphylococcal biofilms. The
277 fluorescence signal was fairly dim when imaging Coa:msfGFP, however, it is not known how much
278 Coa is produced and therefore the concentration could be low. Additionally, we imaged the fusion
279 protein in the complex environment of a biofilm. Biofilms are thick, heterogeneous samples that are
280 autofluorescent and attenuate and distort both the excitation and emission from fluorescent
281 molecules, which makes them a challenging environment to image in. However, the fact that
282 Coa:msfGFP could be visualised by standard CLSM imaging is encouraging, and advanced
283 microscopes with more sensitive detection will facilitate more detailed analyses. For example,
284 single-molecule microscopy on live bacteria has revealed important details of Tat-mediated
285 transport in Gram-negative *E. coli*, and similar investigations could be pursued for Sec-secreted

286 proteins in Gram-positive bacteria using msfGFP fusions [21]. In particular, future studies could
287 utilise total internal reflection fluorescence (TIRF) microscopy to investigate extracellular secretion
288 between the cell and a surface such as an agarose pad or glass coverslip, that are sensitive at single-
289 molecule GFP detection limits in live bacteria [38][39], or faster millisecond Slimfield microscopy
290 that could potentially enable mobility studies of extracellular secreted components [40][41][42].

291 *S. aureus* is a major biofilm-forming human pathogen that establishes infections, causes
292 disease, and evades the immune system through a number of secreted and cell surface associated
293 proteins, many of which contain a Sec-type signal peptide [23]. Fusions with msfGFP will greatly
294 benefit future research into these proteins. We do not know whether msfGFP would be exported
295 correctly via the Sec pathway in other bacterial species; past studies into GFP export via the Tat
296 pathway in Gram positive bacteria revealed that a different GFP variant was not exported correctly
297 in all species tested [6]. The authors speculated that their results were due to differences in the
298 physical or chemical structure of the cell wall, or in the quality control mechanisms of the Tat
299 translocases. Such interspecies differences may also affect the outcome when using msfGFP for Sec
300 exported proteins, and this is important to bear in mind. The assay performed by expression of
301 msfGFP from pRMC2 vector in our study, however, provides an easy tool for checking the
302 feasibility of msfGFP secretion in other *Staphylococci* that are compatible with this vector, and the
303 Tat and Sec signal peptide constructs can be cloned into different vectors for studies in other Gram-
304 positive bacteria.

305 We have confirmed that msfGFP is a good candidate for labelling proteins secreted by the
306 Sec pathway in *S. aureus*. We fused *msfGFP* to *coa* in the *S. aureus* chromosome and demonstrated
307 that fusion to msfGFP did not prevent Coa from functioning correctly, that msfGFP could fold
308 correctly and fluoresce in the extracellular environment, and that the fusion protein localised as
309 expected in the extracellular environment. *S. aureus* utilises a myriad of surface associated and

310 secreted proteins to establish infections and cause disease, and our work opens the door for
311 developing fusion proteins to investigate these and progress our understanding of *S. aureus*
312 infection.

313

314 **MATERIALS AND METHODS**

315 **Materials, bacterial strains, and growth conditions**

316 All bacterial strains, plasmids, and primers used are listed in Table 1. For long-term storage,
317 bacteria were stored in 25 % glycerol at -80 °C. *E. coli* and *S. aureus* were cultured in Luria Broth
318 (LB, L3522, Sigma-Aldrich) and Brain Heart Infusion (BHI, 53286, Millipore), respectively, at 37
319 °C with 180 rpm shaking. When grown on agar, 15 g/L agar (A1296, Sigma-Aldrich) was added to
320 the media. For plasmid selection, the media was supplemented with 25 µg/ml or 10 µg/ml
321 chloramphenicol (Cm, C0378, Sigma-Aldrich), or 100 µg/ml ampicillin (Amp, A9393, Sigma-
322 Aldrich). Biofilms were grown in modified BHI (mBHI) supplemented with 50 % heparin stabilised
323 human plasma to mimic physiological conditions. mBHI is BHI supplemented with 2.1 mM CaCl₂
324 (C3881, Sigma-Aldrich) and 0.4 mM MgCl₂ (31413, Sigma-Aldrich). When low autofluorescence
325 conditions were required, bacteria were suspended in mM9 medium. mM9 is a minimal medium
326 comprising of M9 salts (M6030, Sigma-Aldrich) supplemented with 2 mM MgSO₄ (M1880,
327 Sigma-Aldrich), 0.1 mM CaCl₂ (C3881, Sigma-Aldrich), 1 % glucose (1.08346, Merck), 1 %
328 casamino acids (Gibco, 223050), 1 mM Thiamine-HCl (T4625, Sigma-Aldrich), and 0.05 mM
329 nicotinamide (72340, Sigma-Aldrich) [43]. Plasma was collected from blood donated by Aarhus
330 University Hospital by centrifugation at 2000 x g for 15 minutes at 4 °C and stored in aliquots at -
331 80 °C. Before use, frozen plasma was immediately thawed in a water bath at 37 °C. Tat and Sec

332 signal peptide fusion protein expression was induced with the addition of 340 ng/ml
333 anhydrotetracycline (ATc, 94664, Sigma-Aldrich).

334

335 **Construction of pRMC2 overexpression vector carrying signal peptide:msfGFP constructs**

336 Tat and Sec signal peptide sequences were fused to *msfGFP* to create *tat:msfGFP* and *sec:msfGFP*
337 in the vector pRMC2 (Figure 1), a plasmid with an inducible P_{xyI/tetO} promoter and origin of
338 replication for *E. coli* and *Staphylococci* (Table 1) [44]. A positive control was also constructed
339 expressing *msfGFP* with no signal peptide (Figure 1). Note that the Shine-Dalgarno sequences were
340 added later as described in the following section.

341 Sequences for *msfGFP* [34], Tat [18], and Sec signal peptides [45] were reverse translated
342 with an *S. aureus* USA300 codon usage table (see Supplementary Table S1 for sequences). The
343 RNA polymerase α and β subunits are highly conserved, and their nucleotide sequences were used
344 to predict codon usage in *S. aureus* USA300 and *S. aureus* 29213, and an *S. aureus* USA300 codon
345 usage table was deemed suitable. Signal peptide sequences were ordered as oligos (Thermo Fisher
346 Scientific) and *msfGFP* with a linker at its N-terminal was ordered on a high copy plasmid (pUC57,
347 Genscript). The signal peptide sequences and *msfGFP* were amplified by PCR with Phusion
348 polymerase (F566S, Thermo Fisher Scientific) according to the manufacturer's instructions. The
349 primers (Invitrogen), listed in Table 2, contained overhangs intended to join fragments and add
350 KpnI and EcoRI restriction sites at the 5' and 3' ends. Primers 2Ftg/2Rb and 2Fsg/2Ra were used to
351 amplify Tat and Sec signal peptide sequences, respectively, and *msfGFP* was amplified with
352 1Fa/1Rsg. The signal peptide sequences were joined to *msfGFP* via SOE-PCR to create *tat:msfGFP*
353 (primers 1Fa/Rtg) and *sec:msfGFP* (primers 1Fa/2Ra). *msfGFP* was also amplified alone with no
354 signal peptide sequence to be used as a control. PCR products were analysed by gel electrophoresis

355 and purified with the GenElute Gel Extraction Kit (NA1111, Sigma-Aldrich). All PCR products and
356 pRMC2 were digested by KpnI (FD0524, Thermo Fisher Scientific) and EcoRI (FD0274, Thermo
357 Fisher Scientific), and PCR products were ligated into pRMC2 with T4 DNA ligase (EL0011,
358 Invitrogen) according to the manufacturer's protocols.

359

360 **Insertion of Shine-Dalgarno sequence via site directed mutagenesis**

361 In order to make the translation of *msfGFP* possible, the Shine-Dalgarno sequence was inserted
362 upstream of the signal peptide and *msfGFP* sequences via site directed mutagenesis [46]. The
363 consensus sequence was chosen [47] and inserted 5 nucleotides upstream of the start codons of
364 *tat:msfGFP*, *sec:msfGFP*, and *msfGFP* to ensure maximum translation efficiency [48]. To do this, a
365 mutagenic primer, MutF, was designed with an overhang containing the Shine-Dalgarno sequence
366 and used to amplify the entire pRMC2 constructs containing *tat:msfGFP*, *sec:msfGFP* and *msfGFP*
367 and simultaneously insert the sequence at the desired place. A unique reverse primer was designed
368 for each construct, while the mutagenic primer MutF remained the same (MutF/TatR for
369 *tat:msfGFP*, MutF/SecR for *sec:msfGFP*, and MutF/GfpR for *msfGFP*). The primers were
370 phosphorylated using T4 Polynucleotide Kinase (EK0031, Thermo Fisher Scientific) according to
371 the manufacturer's instructions. The constructs were then amplified using the phosphorylated
372 primers and Phusion polymerase (Phusion Hot Start II DNA Polymerase, F549S, Thermo Fisher
373 Scientific) according to the manufacturer's instructions. The new PCR products were digested with
374 DpnI to remove methylated template DNA, after which the mutated plasmids were ligated back into
375 a whole plasmid according to the manufacturer's instructions (Phusion Site-Directed Mutagenesis
376 Kit, F541, Thermo Fisher Scientific).

377

378 **Transformation into *E. coli* IM08B**

379 The pRMC2 constructs expressing Tat:msfGFP, Sec:msfGFP, or msfGFP, and empty pRMC2, were
380 first transformed via heat shock into *E. coli* IM08B in order to gain a methylation profile mimicking
381 *S. aureus* [49]. To prepare chemical competent cells, an overnight culture of *E. coli* IM08B was
382 diluted to OD₆₀₀ 0.02 and grown to OD₆₀₀ 0.3, then chilled on ice for 10 minutes. Cells were
383 harvested by centrifugation at 4000 x g for 10 minutes at 4 °C and resuspended in 5 ml ice cold 0.5
384 M CaCl₂. The centrifugation was repeated, and the cells resuspended in 1.2 ml 0.5 M CaCl₂ before
385 incubating on ice for 30 minutes. For transformation, 1-3 µl of each pRMC2 construct was
386 incubated for 30 minutes on ice with 50 µl of competent cells. A heat shock was applied at 42 °C
387 for 90 s, and cells were then transferred to ice for 2 minutes. 950 µl of preheated LB media (37 °C)
388 was added and then cells incubated with 180 rpm shaking for 1 hour at 37 °C. Cells were finally
389 plated on agar with Amp and incubated at 37 °C overnight. Plasmids were extracted from positive
390 transformants with the GeneJET Plasmid Miniprep Kit (K0502, Sigma-Aldrich) and sent for
391 sequencing with Macrogen Europe with primers FwdRMC2/RevRMC2.

392

393 **Transformation into *S. aureus* 29213**

394 Plasmids with the correct sequence were transformed into *S. aureus* 29213 by electroporation. To
395 prepare electrocompetent cells, an overnight culture was diluted to OD₆₀₀ 0.5 and grown to OD₆₀₀
396 0.6. Cells were harvested by centrifugation at 4000 x g for 10 minutes at 4 °C and washed in 50 ml
397 ice cold MilliQ water three times. Cells were then centrifuged and resuspended in 50 ml, then 5 ml,
398 2 ml, and finally 0.25 ml ice cold 0.5 M sucrose. Up to 1 µg plasmid DNA was incubated on ice
399 with 50 µl fresh competent cells for 10 minutes before being transferred to a chilled 1 mm
400 electroporation cuvette and electroporated at 2.1 kV, 200 Ω, and 25 µF in an ECM 630 BTXTM

401 (Harvard Apparatus). Immediately afterwards, 1 ml preheated BHI supplemented with 0.5 M
402 sucrose (37 °C) was added to the cells, which were then incubated at 37 °C with 150 rpm shaking
403 for 2 hours. Cells were finally plated on agar containing Cm and incubated overnight at 37 °C.
404 Positive transformants were confirmed by sequencing as described in the prior section.

405

406 **Creation of gene deletion mutants**

407 In-frame single deletions of the *coa* and *vwbp* genes were achieved through splicing by overlap
408 extension PCR according to Monk and colleagues [50] and performed as described in detail in
409 Wassmann et al. 2022 [51]. The double mutant was created by introducing the pIMAY Δ *coa*
410 plasmid into the Δ *vwbp* mutant and deleting the *coa* gene in the Δ *vwbp* mutant.

411

412 **Construction and evaluation of a chromosome-integrated Coa:msfGFP fusion protein**

413 A C-terminal, chromosome-integrated fusion Coa:msfGFP was created by allelic replacement using
414 the protocol from Monk *et al.* [50]. Primers Coa:msfGFP_F/Coa:msfGFP_R were used to amplify
415 *coa:msfGFP* from a pUC57-*msfgfp* and add overhangs for Gibson Assembly. pIMAY was digested
416 using restriction enzyme KpnI (R3142S, New England Biolabs) and then ligated to *coa:msfGFP* via
417 Gibson Assembly [52] using a kit (E5510S, New England Biolabs). The ligated construct was first
418 transformed via chemical transformation into *E. coli* IM08B to gain a methylation profile
419 mimicking that of *S. aureus* [49], and was then extracted and transformed via electroporation into *S.*
420 *aureus* 29213 wildtype and Δ *vwbp*, a mutant lacking vWbp, the other coagulase that *S. aureus*
421 produces [37]. After transformation into *S. aureus*, the plasmid was then integrated into the
422 chromosome and finally the backbone was excised using the protocol from Monk *et al.* [50]. The
423 genotype of the fusion protein was assessed via sequencing with the OutR/OutF primers and the

424 phenotype was assessed via coagulation assays. For coagulation assays, overnight cultures of the
425 mutant and parental strains were diluted to OD₆₀₀ 0.5 in 1 ml of 1:6 heparin-stabilised human
426 plasma in 0.85 % NaCl (w/v) (S5886, Sigma-Aldrich) in sterile glass tubes and incubated for 24
427 hours at 37 °C with no shaking. Coagulation was assessed by tilting and observing the tubes after
428 24 hours incubation. A negative control without bacteria was also included in addition to the mutant
429 lacking both Coa and vWbp, which should not coagulate plasma.

430

431 **Screening for msfGFP fluorescence in cell cultures and supernatants by bulk fluorescence**

432 To verify if msfGFP was successfully secreted by the Tat and Sec pathways, the supernatants of
433 bacteria expressing the signal peptide and msfGFP fusions were investigated for fluorescence by
434 bulk and in-gel measurements. Bacterial cultures and supernatants from *S. aureus* 29213 expressing
435 Tat:msfGFP, Sec:msfGFP, msfGFP, or no msfGFP from the overexpression vector pRMC2 were
436 grown overnight in BHI and diluted to OD₆₀₀ 0.1 in mM9 medium and incubated at 37 °C with 180
437 rpm shaking until OD₆₀₀ 0.5. mM9 was used in place of BHI because it is less autofluorescent. ATc
438 (340 ng/ml) was added to the cultures, after which they were further incubated for 60 minutes to
439 induce the P_{xyl/tetO} promoter and msfGFP expression. Final OD₆₀₀ was recorded, and 2 ml of each
440 sample taken. For the fluorescence bulk measurements, 200 µl was added directly into a 96 well
441 plate (Nunc F96 MicroWell Black-bottom plate, 237105, Thermo Fisher Scientific) and the
442 remaining 1.8 ml was centrifuged at 14104 x g for 10 minutes. The supernatant was removed,
443 sterile filtered with a 0.2 µm filter (83.1826.001, Sarstedt), and 200 µl was added to the 96-well
444 plate. Three biological replicates (from independently grown cultures) and three technical replicates
445 (individually prepared samples from the same culture) were tested per construct. Fluorescence was
446 measured at 488 nm wavelength excitation, 510 nm wavelength emission, and 1000 ms exposure

447 time in a Varioskan Lux Flash Plate Reader (Thermo Fisher Scientific). Median fluorescence values
448 were calculated and normalised to the optical density. The values were tested for normality with a
449 Shapiro-Wilk test, after which they were compared using a one-way ANOVA followed by a
450 Tukey's test with a $p < 0.05$ significance level.

451

452 **Visualisation of secreted msfGFP and Coa:msfGFP via in-gel fluorescence**

453 To verify whether Sec:msfGFP and Tat:msfGFP were secreted and folded correctly, and to confirm
454 whether Coa:msfGFP was secreted as an intact, functionally fluorescent protein, we separated the
455 supernatant on a native PAGE gel. Cultures that expressed either Coa:msfGFP, Tat:msfGFP,
456 msfGFP, an empty vector were grown to the exponential phase in mM9, and the chromosome-
457 integrated Coa:msfGFP cultures were grown to the stationary phase in BHI, after which the
458 supernatant was collected and either stored at $-80\text{ }^{\circ}\text{C}$ or used right away. The supernatants were
459 mixed 1:1 with a native sample buffer (1610738, Bio-Rad) and separated on a 4–15 % precast
460 polyacrylamide protein gel (Mini-PROTEAN TGX, 4561086, Bio-Rad). Coa-msfGFP and
461 fluorescence was detected in the Amersham Typhoon Scanner (29187191, Cytiva) with a 488 nm
462 excitation and 510 nm emission. A His-tagged GFP (14-392, Sigma-Aldrich) was also loaded on
463 the gel and used as a positive control for GFP fluorescence as well as a size marker.

464

465 **Confocal microscopy of *S. aureus* expressing signal peptide fusions**

466 To visualise whether msfGFP was retained within cells, all overexpression constructs were also
467 imaged with confocal laser scanning microscopy (CLSM). Overnight cultures were diluted to OD_{600}
468 0.1 in mM9 medium and were grown to OD_{600} 0.5, then incubated for a further 2 hours with 340
469 ng/ml ATc and imaged with the LSM700 confocal microscope (Zeiss) with a 10 mW 488nm

470 wavelength laser at 2 % power and a Plan-Apochromat 63x/1.40 NA oil immersion objective lens.
471 Images were captured with the Axiocam HR camera (Zeiss) and using the Zen Black software
472 (Zeiss).

473

474 **Confocal microscopy of *S. aureus* expressing Coa:msfGFP**

475 *S. aureus* expressing either the chromosome-integrated fusion Coa:msfGFP or unmodified Coa
476 were grown overnight in BHI and then diluted to OD₆₀₀ 5. Microwells (μ -Slide 8 Well, 80821,
477 IBIDI) were preconditioned with 180 μ l BHI supplemented with 50 % plasma, 10 μ M Syto41
478 (S11352, Invitrogen), and 0.4 μ g/ml Alexa Fluor 647-conjugated fibrinogen (F35200, Invitrogen)
479 by incubating at 37 °C for 30 minutes. Then 20 μ l OD₆₀₀ 5 cultures were added and incubated for a
480 further 2 hours. The biofilms were imaged with 405 nm, 488 nm, and 639 nm wavelength excitation
481 and a Plan-Apochromat 63x/1.40 NA oil immersion objective in the LSM700 confocal microscope
482 (Zeiss). Images were captured with the Axiocam HR camera (Zeiss) and using the Zen Black
483 software (Zeiss). GFP fluorescence was detected with 488 nm wavelength excitation and 490-600
484 nm wavelength emission, and Alexa 647-conjugated fibrinogen was detected with 639 nm
485 wavelength excitation and 640-750 nm emission.

486

487 **ACKNOWLEDGEMENTS**

488 ML was supported by the BBSRC (BB/R001235/1), EPSRC (EP/T002166/1), the Leverhulme Trust
489 (RPG-2017-340), and the Carlsberg Foundation (CF16-0342). We thank Melissa Eriksen for
490 assisting in primer design. The authors declare no conflicts of interest.

491

492 **REFERENCES**

- 493 [1] Chiu SW and Leake MC (2011). Functioning nanomachines seen in real-time in living bacteria
494 using single-molecule and super-resolution fluorescence imaging. **Int. J. Mol. Sci.** 12(4): 2518–
495 2542. doi: 10.3390/ijms12042518
- 496 [2] Chudakov DM, Matz MV, Lukyanov S, and Lukyanov KA (2010). Fluorescent proteins and
497 their applications in imaging living cells and tissues. **Physiol. Rev.** 90(3): 1103–1163. doi:
498 10.1152/physrev.00038.2009
- 499 [3] Linton E, Walsh MK, Sims RC, and Miller CD (2012). Translocation of green fluorescent
500 protein by comparative analysis with multiple signal peptides. **Biotechnol. J.** 7(5): 667–676. doi:
501 10.1002/biot.201100158
- 502 [4] Thomas JD, Daniel RA, Errington J, and Robinson C (2001). Export of active green fluorescent
503 protein to the periplasm by the twin-arginine translocase (Tat) pathway in Escherichia coli. **Mol.**
504 **Microbiol.** 39(1): 47–53. doi: 10.1046/j.1365-2958.2001.02253.x
- 505 [5] Li SY, Chang BY, and Lin SC (2006). Coexpression of TorD enhances the transport of GFP via
506 the TAT pathway. **J. Biotechnol.** 122(4): 412–421. doi: 10.1016/j.jbiotec.2005.09.011
- 507 [6] Meissner D, Vollstedt A, Van Dijl JM, and Freudl R (2007). Comparative analysis of twin-
508 arginine (Tat)-dependent protein secretion of a heterologous model protein (GFP) in three different
509 Gram-positive bacteria. **Appl. Microbiol. Biotechnol.** 76(3): 633–642. doi: 10.1007/s00253-007-
510 0934-8
- 511 [7] van der Ploeg R, Monteferrante CG, Piersma S, Barnett JP, Kouwen TR, Robinson C, and van
512 Dijl JM (2012). High-salinity growth conditions promote tat-independent secretion of tat substrates
513 in Bacillus subtilis. **Appl. Environ. Microbiol.** 78(21): 7733–7744. doi: 10.1128/AEM.02093-12

- 514 [8] Snyder AJ, Mukherjee S, Glass JK, Kearns DB, and Mukhopadhyay S (2014). The canonical
515 twin-arginine translocase components are not required for secretion of folded green fluorescent
516 protein from the ancestral strain of bacillus subtilis. **Appl. Environ. Microbiol.** 80(10): 3219–3232.
517 doi: 10.1128/AEM.00335-14
- 518 [9] Guo L, Wu T, Hu W, He X, Sharma S, Webster P, Gimzewski JK, Zhou X, Lux R, and Shi W
519 (2013). Phenotypic characterization of the foldase homologue PrsA in Streptococcus mutans. **Mol.**
520 **Oral Microbiol.** 28(2): 154–165. doi: 10.1111/omi.12014
- 521 [10] Cowley SC and Av-Gay Y (2001). Monitoring promoter activity and protein localization in
522 Mycobacterium spp. using green fluorescent protein. **Gene** 264(2): 225–231. doi: 10.1016/S0378-
523 1119(01)00336-5
- 524 [11] Hoffmann A, Schneider T, Pag U, and Sahl HG (2004). Localization and functional analysis of
525 PepI, the immunity peptide of Pep5-producing Staphylococcus epidermidis strain 5. **Appl.**
526 **Environ. Microbiol.** 70(6): 3263–3271. doi: 10.1128/AEM.70.6.3263-3271.2004
- 527 [12] Knapp A, Rippahn M, Volkenborn K, Skoczinski P, and Jaeger KE (2017). Activity-
528 independent screening of secreted proteins using split GFP. **J. Biotechnol.** 258: 110–116. doi:
529 10.1016/j.jbiotec.2017.05.024
- 530 [13] Wiedenmann J, Oswald F, and Nienhaus GU (2009). Fluorescent proteins for live cell imaging:
531 Opportunities, limitations, and challenges. **IUBMB Life** 61(11): 1029–1042. doi: 10.1002/iub.256
- 532 [14] Prabudiansyah I, Driessen AJM (2017). The Canonical and Accessory Sec System of Gram-
533 positive Bacteria. **Curr Top Microbiol Immunol.** 404: 45-67. doi: 10.1007/82_2016_9
- 534 [15] Green ER and Meccas J (2016). Bacterial Secretion Systems: An Overview. **Microbiol.**
535 **Spectr.** 4(1): 1–19. doi: 10.1128/microbiolspec.vmbf-0012-2015

- 536 [16] Papanikou E, Karamanou S, and Economou A (2007). Bacterial protein secretion through the
537 translocase nanomachine. **Nat. Rev. Microbiol.** 5(11): 839–851. doi: 10.1038/nrmicro1771
- 538 [17] Robinson C and Bolhuis A (2004). Tat-dependent protein targeting in prokaryotes and
539 chloroplasts. **Biochim. Biophys. Acta - Mol. Cell Res.** 1694(1-3): 135–147. doi:
540 10.1016/j.bbamcr.2004.03.010
- 541 [18] Biswas L, Biswas R, Nerz C, Ohlsen K, Schlag M, Schäfer T, Lamkemeyer T, Ziebandt AK,
542 Hantke K, Rosenstein R, Götz F (2009). Role of the twin-arginine translocation pathway in
543 *Staphylococcus*. **J. Bacteriol.** 191(19): 5921–5929. doi: 10.1128/JB.00642-09
- 544 [19] Müller M (2005). Twin-arginine-specific protein export in *Escherichia coli*. **Res. Microbiol.**
545 156(2): 131–136. doi: 10.1016/j.resmic.2004.09.016
- 546 [20] Berks BC, Palmer T, and Sargent F (2005). Protein targeting by the bacterial twin-arginine
547 translocation (Tat) pathway. **Curr. Opin. Microbiol.** 8(2): 174–181. doi:
548 10.1016/j.mib.2005.02.010
- 549 [21] Leake MC, Greene NP, Godun RM, Granjon T, Buchanan G, Chen S, Berry RM, Palmer T,
550 and Berks BC (2008). Variable stoichiometry of the TatA component of the twin-arginine protein
551 transport system observed by in vivo single-molecule imaging. **Proc. Natl. Acad. Sci. U. S. A.**
552 105(40): 15376–15381. doi: 10.1073/pnas.0806338105
- 553 [22] Tong SYC, Davis JS, Eichenberger E, Holland TL, and Fowler VG (2015). *Staphylococcus*
554 *aureus* infections: Epidemiology, pathophysiology, clinical manifestations, and management. **Clin.**
555 **Microbiol. Rev.** 28(3): 603–661. doi: 10.1128/CMR.00134-14

556 [23] Foster TJ, Geoghegan JA, Ganesh VK, and Höök M (2014). Adhesion, invasion and evasion:
557 The many functions of the surface proteins of *Staphylococcus aureus*. **Nat. Rev. Microbiol.** 12(1):
558 49–62. doi: 10.1038/nrmicro3161

559 [24] Crosby HA, Kwiecinski J, Horswill AR, Roy J, and City I (2016). *Staphylococcus aureus*
560 aggregation and coagulation mechanisms, and their function in host-pathogen interactions. **Adv.**
561 **Appl. Microbiol.** 96: 1–41. doi: 10.1016/bs.aambs.2016.07.018.Staphylococcus

562 [25] Stapels DA, Ramyar KX, Bischoff M, von Köckritz-Blickwede M, Milder FJ, Ruyken M,
563 Eisenbeis J, McWhorter WJ, Herrmann M, van Kessel KP, Geisbrecht BV, and Rooijackers SH
564 (2014). *Staphylococcus aureus* secretes a unique class of neutrophil serine protease inhibitors. **Proc.**
565 **Natl. Acad. Sci. U. S. A.** 111(36): 13187–13192. doi: 10.1073/pnas.1407616111

566 [26] Hussain M, Becker K, Von Eiff C, Schrenzel J, Peters G, and Herrmann M (2001).
567 Identification and characterization of a novel 38.5-Kilodalton cell surface protein of *Staphylococcus*
568 *aureus* with extended-spectrum binding activity for extracellular matrix and plasma proteins. **J.**
569 **Bacteriol.** 183(23): 6778–6786. doi: 10.1128/JB.183.23.6778-6786.2001

570 [27] Ko YP, Kuipers A, Freitag CM, Jongerius I, Medina E, van Rooijen WJ, Spaan AN, van
571 Kessel KP, Höök M, Rooijackers SH (2013). Phagocytosis Escape by a *Staphylococcus aureus*
572 Protein That Connects Complement and Coagulation Proteins at the Bacterial Surface. **PLoS**
573 **Pathog.** 9(12): 1–13. doi: 10.1371/journal.ppat.1003816

574 [28] Palma M, Nozohoor S, Schennings T, Heimdahl A, and Flock JI (1996). Lack of the
575 extracellular 19-kilodalton fibrinogen-binding protein from *Staphylococcus aureus* decreases
576 virulence in experimental wound infection. **Infect. Immun.** 64(12): 5284–5289. doi:
577 10.1128/iai.64.12.5284-5289.1996

- 578 [29] McAdow M, Missiakas DM, and Schneewind O (2012). Staphylococcus aureus secretes
579 coagulase and von willebrand factor binding protein to modify the coagulation cascade and
580 establish host infections. **J. Innate Immun.** 4(2): 141–148. doi: 10.1159/000333447
- 581 [30] Guggenberger C, Wolz C, Morrissey JA, and Heesemann J (2012). Two distinct coagulase-
582 dependent barriers protect Staphylococcus aureus from neutrophils in a three dimensional in vitro
583 infection model. **PLoS Pathog.** 8(1). doi: 10.1371/journal.ppat.1002434
- 584 [31] Cheng AG, Mcadow M, Kim HK, Bae T, and Missiakas DM (2010). Contribution of
585 Coagulases towards Staphylococcus aureus Disease and Protective Immunity. **PLoS Pathog.** 6(8).
586 doi: 10.1371/journal.ppat.1001036
- 587 [32] Vanassche T, Verhaegen J, Peetermans WE, VAN Ryn J, Cheng A, Schneewind O, Hoylaerts
588 MF, Verhamme P (2011). Inhibition of staphylothrombin by dabigatran reduces Staphylococcus
589 aureus virulence. **J. Thromb. Haemost.** 9: 2436–2446. doi: 10.1111/j.1538-7836.2011.04529.x
- 590 [33] Reth M (2013). Matching cellular dimensions with molecular sizes. *Nature Immunol.* 14: 765-
591 767. doi: 10.1038/ni.2621
- 592 [34] Ke N, Landgraf D, Paulsson J, and Berkmen M (2016). Visualization of periplasmic and
593 cytoplasmic proteins with a self-labeling protein tag. **J. Bacteriol.** 198(7): 1035–1043. doi:
594 10.1128/JB.00864-15
- 595 [35] Sibbald MJ, Ziebandt AK, Engelmann S, Hecker M, de Jong A, Harmsen HJ, Raangs GC,
596 Stokroos I, Arends JP, Dubois JY, van Dijl JM (2006). Mapping the Pathways to Staphylococcal
597 Pathogenesis by Comparative Secretomics. **Microbiol. Mol. Biol. Rev.** 70(3): 755–788. doi:
598 10.1128/mmbr.00008-06

- 599 [36] Scholz O, Schubert P, Kintrup M, and Hillen W (2000). Tet repressor induction without Mg²⁺.
600 **Biochemistry** 39(35): 10914–10920. doi: 10.1021/bi001018p
- 601 [37] Bjerketorp J, Nilsson M, Ljungh Å, Flock JI, Jacobsson K, and Frykberg L (2002). A novel
602 von Willebrand factor binding protein expressed by *Staphylococcus aureus*. **Microbiology** 148:
603 2037–2044. doi: 10.1099/00221287-148-7-2037
- 604 [38] Leake MC, Chandler JH, Wadhams GH, Bai F, Berry RM, and Armitage JP (2006).
605 Stoichiometry and turnover in single, functioning membrane protein complexes. **Nature** 443(7109):
606 355–358. doi: 10.1038/nature05135
- 607 [39] Delalez NJ, Wadhams GH, Rosser G, Xue Q, Brown MT, Dobbie IM, Berry RM, Leake MC,
608 and Armitage JP (2010). Signal-dependent turnover of the bacterial flagellar switch protein FliM.
609 **Proc. Natl. Acad. Sci. U. S. A.** 107(25): 11347–11351. doi: 10.1073/pnas.1000284107
- 610 [40] Plank M, Wadhams GH, and Leake MC (2009). Millisecond timescale slimfield imaging and
611 automated quantification of single fluorescent protein molecules for use in probing complex
612 biological processes. **Integr. Biol.** 1(10): 602–612. doi: 10.1039/b907837a
- 613 [41] Reyes-Lamothe R, Sherratt DJ, and Leake MC (2010). Stoichiometry and architecture of active
614 DNA replication machinery in *Escherichia coli*. **Science** 328(5977): 498–501. doi:
615 10.1126/science.1185757
- 616 [42] Jin X, Lee JE, Schaefer C, Luo X, Wollman AJM, Payne-Dwyer AL, Tian T, Zhang X, Chen
617 X, Li Y, McLeish TCB, Leake MC, and Bai F (2021). Membraneless organelles formed by liquid-
618 liquid phase separation increase bacterial fitness. **Sci. Adv.** 7(43): doi: 10.1126/sciadv.abh2929
- 619 [43] Reed P, Atilano ML, Alves R, Hoiczkyk E, Sher X, Reichmann NT, Pereira PM, Roemer T,
620 Filipe SR, Pereira-Leal JB, Ligoxygakis P, and Pinho MG (2015). *Staphylococcus aureus* Survives

621 with a Minimal Peptidoglycan Synthesis Machine but Sacrifices Virulence and Antibiotic
622 Resistance. **PLoS Pathog.** 11(5): 1–19. doi: 10.1371/journal.ppat.1004891

623 [44] Corrigan RM and Foster TJ (2009). An improved tetracycline-inducible expression vector for
624 *Staphylococcus aureus*. **Plasmid** 61(2): 126–129. doi: 10.1016/j.plasmid.2008.10.001

625 [45] Schallenberger MA, Niessen S, Shao C, Fowler BJ, and Romesberg FE (2012). Type I signal
626 peptidase and protein secretion in *Staphylococcus aureus*. **J. Bacteriol.** 194(10): 2677–2686. doi:
627 10.1128/JB.00064-12

628 [46] Kunkel TA (1985). Rapid and efficient site-specific mutagenesis without phenotypic selection.
629 **Proc. Natl. Acad. Sci. U. S. A.** 82(2): 488–492. doi: 10.1073/pnas.82.2.488

630 [47] Vimberg V, Tats A, Remm M, and Tenson T (2007). Translation initiation region sequence
631 preferences in *Escherichia coli*. **BMC Mol. Biol.** 8: 1–13. doi: 10.1186/1471-2199-8-100

632 [48] McLaughlin JR, Murray CL, and Rabinowitz JC (1981). Unique features in the ribosome
633 binding site sequence of the gram-positive *Staphylococcus aureus* β -lactamase gene. **J. Biol. Chem.**
634 256(21): 11283–11291. doi: 10.1016/S0021-9258(19)68589-3

635 [49] Monk IR, Tree JJ, Howden BP, Stinear TP, and Foster TJ (2015). Complete bypass of
636 restriction systems for major *Staphylococcus aureus* lineages. **MBio** 6(3): 1–12. doi:
637 10.1128/mBio.00308-15

638 [50] Monk IR, Shah IM, Xu M, Tan MW, and Foster TJ (2012). Transforming the untransformable:
639 Application of direct transformation to manipulate genetically *Staphylococcus aureus* and
640 *Staphylococcus epidermidis*. **MBio** 3(2): 1–11. doi: 10.1128/mBio.00277-11

641 [51] Wassmann CS, Rolsted AP, Lyngsie MC, Torres-Puig S, Kronborg T, Vestergaard M, Ingmer
642 H, Pontoppidan SP, Klitgaard JK (2022). The menaquinone pathway is important for susceptibility

643 of *Staphylococcus aureus* to the antibiotic adjuvant, cannabidiol. **Microbiol. Res.** 257. doi:

644 10.1016/j.micres.2022.126974

645 [52] Gibson DG, Young L, Chuang RY, Venter JC, Hutchison CA, and Smith HO (2009).

646 Enzymatic assembly of DNA molecules up to several hundred kilobases. **Nat. Methods** 6(5): 343–

647 345. doi: 10.1038/nmeth.1318

648 [53] Boden MK and Flock JI (1989). Fibrinogen-binding protein/clumping factor from

649 *Staphylococcus aureus*. **Infection and Immunity** 57(8): 2358-2363. doi: 10.1128/iai.57.8.2358-

650 2363.1989

651 [54] Qazi SNA, Rees CED, Mellits KH, and Hill PJ (2001). Development of gfp vectors for

652 expression in *Listeria monocytogenes* and other low G+C gram positive bacteria. **Microb. Ecol.**

653 41(4): 301–309. doi: 10.1007/s002480000091

654

655 **FIGURE AND TABLE LEGENDS**

656 Table 1 Bacterial strains and plasmids used in this study.

657

658 Table 2 Primers used in this study. Annealing sequence of primers is given in upper case, and

659 overhangs in lower case text.

660

661 **Tables**

662 Table 1

Bacterial Strain	Description	Reference
<i>Escherichia coli</i> IM08B	mcrA Δ(mrr-hsdRMS-mcrBC) φ80lacZΔM15 ΔlacX74 recA1 araD139 Δ(ara-leu)7697 galU galK rpsL endA1 nupG Δdcm ΩPhelp-hsdMS (CC8-2) ΩPN25-hsdS (CC8-1). Derived from <i>E. coli</i> K12 DH10B. Deficient in cytosine methylation (Δdcm) and methylates adenine (<i>hsdMS</i>) to bypass <i>S. aureus</i> restriction barriers	[49]
<i>Staphylococcus aureus</i> 29213 WT	<i>Staphylococcus aureus</i> subsp. <i>aureus</i> Rosenbach (ATCC29213)	www.atcc.org
<i>Staphylococcus aureus</i> Δ <i>vwbp</i>	<i>Staphylococcus aureus</i> subsp. <i>aureus</i> Rosenbach (ATCC29213) (with <i>vwbp</i> gene deleted from the chromosome)	This study
<i>Staphylococcus aureus</i> Δ <i>coa</i> Δ <i>vwbp</i>	<i>Staphylococcus aureus</i> subsp. <i>aureus</i> Rosenbach (ATCC29213) (with <i>coa</i> and <i>vwbp</i> genes deleted from the chromosome)	This study
<i>S. aureus</i> <i>coa:msfGFP</i>	<i>Staphylococcus aureus</i> subsp. <i>aureus</i> Rosenbach (ATCC29213) with Coa:msfGFP genomically integrated fusion protein.	This study
<i>S. aureus</i> ATCC 29213 Δ <i>vwbp</i> <i>coa:msfGFP</i>	<i>Staphylococcus aureus</i> subsp. <i>aureus</i> Rosenbach (ATCC29213) Δ <i>vwbp</i> with Coa:msfGFP genomically integrated fusion protein.	This study
Plasmid	Description	Reference
pRMC2	<i>E. coli</i> / <i>S. aureus</i> shuttle plasmid with inducible promoter P _{xyI/tetO} . Amp ^r , Cm ^r . pRMC2 was a gift from Tim Foster Addgene (http://n2t.net/addgene:68940 ; RRID:Addgene_68940).	[44]
pUC57- <i>msfGFP</i>	<i>E. coli</i> plasmid carrying <i>msfGFP</i> and <i>coa:msfGFP</i> . Amp ^r	Genscript
pIMAY	<i>E. coli</i> /Staphylococci temperature sensitive vector for allelic exchange. Cm ^r . Inducible <i>secY</i> antisense. pIMAY was a gift from Ian Monk. (Also available at Addgene plasmid # 68939 ; http://n2t.net/addgene:68939 ; RRID:Addgene_68939).	[50]
pRMC2- <i>msfGFP</i>	pRMC2 with Shine-Dalgarno sequence and <i>msfGFP</i> inserted downstream from P _{xyI/tetO} promoter. Optimised for <i>S. aureus</i> codon usage. Deposited in Addgene: Plasmid # 194913	This study
pRMC2- <i>sec:msfGFP</i>	pRMC2 with Shine-Dalgarno sequence and Sec signal peptide sequence fused to <i>msfGFP</i> inserted downstream from P _{xyI/tetO} promoter. Optimised for <i>S. aureus</i> codon usage. Deposited in Addgene: Plasmid # 194914	This study
pRMC2- <i>tat:msfGFP</i>	pRMC2 with Shine-Dalgarno sequence and Tat signal peptide sequence fused to <i>msfGFP</i> inserted downstream from P _{xyI/tetO} promoter. Optimised for <i>S. aureus</i> codon usage. Deposited in Addgene: Plasmid # 194915	This study

663

664

665 Table 2

Primer	Sequence (5' – 3') and description	Reference
FwdRMC2	CTCTTCGCTATTACGCCAGC Anneals to pRMC2 multiple cloning site.	This study
RevRMC2	TGGATCCCCTCGAGTTCATG Anneals to pRMC2 multiple cloning site.	This study
1Fa	ttctgaattcttaTTTATATAATTCATCCATACCATGTG Anneals to <i>msfGFP</i> . EcoRI overhang.	This study
1Rsg	gtatcattcagcacatgcaTCAGGTGGTGGAGGATC Anneals to <i>msfGFP</i> . Sec signal peptide overhang.	This study
2Fsg	gatcctccaccacctgaTGCATGTGCTGAATGATAC Anneals to Sec signal peptide sequence. <i>msfGFP</i> overhang.	This study
2Ra	ttctgtaccATGAAAAAATGTATTAACATTATTTTT Anneals to Sec signal peptide sequence. KpnI overhang.	This study
1Rtg	gtgttgcaattggtgcaTCAGGTGGTGGAGGATC Anneals to <i>msfGFP</i> . Tat signal peptide sequence overhang.	This study
2Ftg	gatcctccaccacctgaTGCACCAATTGCAACAC Anneals to Tat signal peptide sequence. <i>msfGFP</i> overhang.	This study
2Rb	ttctgtaccATGACAAATTATGAACAAGTTAATGA Anneals to Tat signal peptide sequence. KpnI overhang.	This study
1Rc	ttctgtaccatgTCAAAGGTGAAGAATTATTTAC Anneals to <i>msfGFP</i> (excluding linker). KpnI restriction site.	This study
MutF	cctcctCATCAAGCTTATTTTAATTATACTC Mutagenic primer containing Shine-Dalgarno sequence.	This study
GfpR	GTACCATGAAAAAATGTATTAAC Reverse mutagenic primer for <i>msfGFP</i> control.	This study
SecR	GTACCATGACAAATTATGAAC Reverse mutagenic primer for <i>sec:msfGFP</i> .	This study
TatR	GTACCATGAAAAAATGTATTAAC Reverse mutagenic primer for <i>tat:msfGFP</i> .	This study
Coa:msfGFP_F	actaaaggaacaaaagctgggtacGGTACCGCCAAGTGAAAC Anneals to Coa:msfGFP construct. pIMAY overhang for Gibson Assembly.	This study
Coa:msfGFP_R	tcgacctcgagggggggcccgtacGGTACCAAATTTTATGAATCGA AG Anneals to Coa:msfGFP construct. pIMAY overhang for Gibson Assembly.	This study
IM151	TACATGTCAAGAATAAACTGCCAAAGC Anneals to pIMAY multiple cloning site.	[50]
IM152	AATACCTGTGACGGAAGATCACTTCG Anneals to pIMAY multiple cloning site.	[50]
OutF	GTGAAATATAGAGATGCTGGTACA Forward primer for screening <i>coa:msfGFP</i> integration	This study
OutR	TGAAGTAGGCTGAAGTTGAAGC Reverse primer for screening <i>coa:msfGFP</i> integration	This study
coa Out F	GTGCGTATAGCGGATTTTGC	This study
coa A	GGGGGTCGACGTGCGCAGCTAAAATATCGCG	This study
coa B	CCTCCAAAATGTAATTGCCCAATC	This study

coa C	GATTGGGCAATTACATTTTGGAGGTCTATCCAAAGACA TACAGTCAA	This study
coa D	GGGGAGCTCGCGGGTTGAAGCAATTCGTTT	This study
coa Out R	CGTTAGGTTATTGAATGAAGTAGG	This study
vwb Out F	GCGAGTGATTCAGACTCAGGTAGTG	This study
vwb A	GGGGGCGGCCGCGATTCAACGAGTGACACAGGATCAG	This study
vwb B	CCTTACACCCTATTTTTTCGCCAAGCC	This study
vwb C	GGCTTGGCGAAAAAATAGGGTGTAAGGGGCTGCAA AGCAAATAATGAGTTTGTCTG	This study
vwb D	GGGGGCGGCCGCGTCAACACTCTCTGTCACTGATGC	This study
vwb Out R	CTAGCTGCCGATGAATCTACAATCTTATTC	This study

666

667

668

669

670

671 **Supplemental information - GFP fusions of Sec-routed extracellular proteins in**
672 ***Staphylococcus aureus* and reveals surface-associated coagulase in biofilms**

673

674 Table S1 Sequences relating to the fusion proteins in this study.

Name	Sequence (5' to 3')	
Shine-Dalgarno	aggagg	[47]
Tat signal peptide	atgacaaattatgaacaagttaatgattcaacacaatttcacgtcgtacattttaaaaatgtaggtattggagg tgcaggtgtgcaattgggca	[18]
Sec signal peptide	atgaaaaaatgtattaaacattattttatcaattattttagttgtatgtcaggttggtatcattcagcacatgca	[45]
Linker	tcaggtggaggagga	
msfGFP	tcaaaagggtgaagaattatttacaggtgttcccaattttagttgaattagatggatgtaatggtcataaattt tcagttcgtgggaagggtgaaggatgcaacaaatgtaaattaacattaaaattattgtacaacaggtaaa ttaccagttccatggccaacattagttacaacattaacatattggtgttcaatgttttcacgttatccagatcatatg aaacaacatgatttttaaatcagcaatgccagaagggtatgtcaagaacgtacaattcatttaaagatgatg gtacatataaaacacgtgcagaagttaaattgaagggtatacattagttaatcgtattgaattaaaaggattga tttaaagaagatggtaataattttaggtcataaattagaatataattttaattcacataatgtttatattacagcagat aaacaaaaaatggtattaaagcaatttaaaattcgtcataatgttgaagatgggtcagttcaattagcagatc attatcaacaaaatacacaattgggtgatggccagttttattaccagataatcattattatcaacacaatcaaaa ttatcaaaagatccaaatgaaaaacgtgatcatatggttttattagaatttgggtacagcagcaggtattacacatg gtatggatgaattatataaa	[34]

675

676